



Original Research

An upward 9.4 T static magnetic field inhibits DNA synthesis and increases ROS-P53 to suppress lung cancer growth



Xingxing Yang^{a,b,1}, Chao Song^{a,b,1}, Lei Zhang^{a,1}, Junjun Wang^{a,c}, Xin Yu^{a,b}, Biao Yu^{a,b}, Vitalii Zablotskii^{d,e}, Xin Zhang^{a,b,c,e,*}

^a CAS Key Laboratory of High Magnetic Field and Ion Beam Physical Biology, High Magnetic Field Laboratory, Hefei Institutes of Physical Science, Chinese Academy of Sciences, Hefei, Anhui 230031, China

^b Science Island Branch of Graduate School, University of Science and Technology of China, Hefei, Anhui 230026, China

^c Institutes of Physical Science and Information Technology, Anhui University, Hefei 230601, China

^d Institute of Physics of the Czech Academy of Sciences, Prague 18221, Czechia

^e International Magnetobiology Frontier Research Center (iMFR), Science Island, 230031, China

ARTICLE INFO

Keywords:

9.4 T static magnetic field (SMF)

Lung cancer

Cell cycle

P53

ROS

ABSTRACT

Studies have shown that 9.4 Tesla (9.4 T) high-field magnetic resonance imaging (MRI) has obvious advantages in improving image resolution and capacity, but their safety issues need to be further validated before their clinical approval. Meanwhile, emerging experimental evidences show that moderate to high intensity Static Magnetic Fields (SMFs) have some anti-cancer effects.

We examined the effects of two opposite SMF directions on lung cancer bearing mice and found when the lung cancer cell-bearing mice were treated with 9.4 T SMFs for 88 h in total, the upward 9.4 T SMF significantly inhibited A549 tumor growth (tumor growth inhibition=41%), but not the downward 9.4 T SMF. *In vitro* cellular analysis shows that 9.4 T upward SMF treatment for 24 h not only inhibited A549 DNA synthesis, but also significantly increased ROS and P53 levels, and arrested G2 cell cycle. Moreover, the 9.4 T SMF-treatments for 88 h had no severe impairment to the key organs or blood cell count of the mice.

Our findings demonstrated the safety of 9.4 T SMF long-term exposure for their future applications in MRI, and revealed the anti-cancer potential of the upward direction 9.4 T SMF.

Introduction

Although the range of SMF of MRI instruments used in most hospitals is about 0.5–3 T, people have already developed high-field MRI because higher field SMF can enable better image resolution and more accurate diagnosis. In fact, in recent few years, 7 T MRI has already been approved by FDA, 9.4 T MRI has also been used in clinical studies [1–4]. Moreover, MRI scanners of >10 T for human and >20 T for rodents are also developed. However, related safety issues of these ultra-high field MRI still need further validation before their eventual application in clinics.

In the meantime, there are multiple studies showing that moderate to high intensity SMFs have some anti-cancer potentials. For example, the proliferation of multiple types of cancer cells could be inhibited by

SMFs in a cell type- and cell plating density- dependent way [5–7]. In fact, emerging data suggested that higher intensity SMFs could often generate more obvious biological effects [8–11]. For example, Higashi et al. found that 4 T SMF could orient almost 100% of red blood cells, while 1 T could only align less than 20% [8]. The p-JNK level of rat cortical neuron cells was increased by 2 T and 5 T SMF treatment, but not 0.1 T–1 T [9]. Recently, we found that 9 T SMF had a more significant effect on cell number reduction than 1 T in HCT116 and CNE-2Z cancer cells, and the EGFR orientation changes and autophosphorylation inhibition were both directly correlated with SMF intensities [10]. In addition, we also found that 27 T SMF could change the mitotic spindle orientation of CNE-2Z cells in a few hours, while 9 T SMF needed 3 days to generate similar phenotype. In contrast, 0.05 T or 1 T SMF could not change the spindle orientation even after 7 days of exposure [11].

Abbreviations: T, tesla; SMF, static magnetic field; MRI, magnetic resonance imaging; ROS, reactive oxygen species; CDK1, cyclin dependent kinase 1; pH3, phospho-histone 3; TGI, tumor growth inhibition effect; TOP2 α , topoisomerase II Alpha; BrdU, 5-bromo-2'-deoxyuridine.

* Corresponding author at: CAS Key Laboratory of High Magnetic Field and Ion Beam Physical Biology, High Magnetic Field Laboratory, Hefei Institutes of Physical Science, Chinese Academy of Sciences, Hefei, Anhui 230031, China.

E-mail address: xinzhang@hmfl.ac.cn (X. Zhang).

¹ These authors contributed equally to this work.

<https://doi.org/10.1016/j.tranon.2021.101103>

Received 17 September 2020; Received in revised form 8 March 2021; Accepted 12 April 2021

1936-5233/© 2021 The Authors. Published by Elsevier Inc. This is an open access article under the CC BY-NC-ND license

(<http://creativecommons.org/licenses/by-nc-nd/4.0/>)

These studies all show that SMFs with higher intensity could affect cells more effectively than lower intensities. Moreover, other than magnetic field intensity, there are multiple evidences showing that the magnetic field direction is also a key factor. More specifically, experiments show that the upward direction and downward direction SMFs could produce differential effects on cells, plants and mice [6, 12–15].

To get a comprehensive understanding about the safety and anti-cancer capacity of high-field SMFs, as well as the impact of magnetic field directions, we constructed incubation systems that can accommodate mice and cells in a vertical superconducting magnetic, which provides 9.4 T homogenous SMF in the center region. We chose 9.4 T because 9.4 T MRI has been initially investigated in a few studies and showed promising image advantages [1–4, 16]. It is expected to be clinically approved in the future, if there are no safety issues. Therefore, we chose 9.4 T not only for its anti-cancer potential, but also for its relevance to the next-generation MRI. Moreover, by switching the electric current direction, we could compare the effects of SMFs of two opposite directions. Our results show that the vertically upward 9.4 T SMF inhibited lung cancer A549 cell proliferation by 31.2% after only one-day exposure ($P < 0.05$). Moreover, 88 h 9.4 T SMF exposure did not cause organ damage to the lung tumor-bearing mice, instead, it significantly inhibited the tumor growth by 44.7% ($P < 0.05$), which reveals the biocompatibility and anti-cancer potentials of high SMF in mice.

Materials and methods

Cell culture

Human lung cancer A459 cells, retinal pigment epithelial RPE1 cells and embryonic kidney 293T cells were all from ATCC. A549 cells were cultured in F12K Nutrient Mixture (#21127-022 Gibco) supplemented with 10% FBS and 1% P/S. RPE1 and 293T cells were cultured in DMEM (10-014-CV, CORNING) supplemented with 10% FBS and 1% P/S. They were all maintained at 37 °C under 5% CO₂ in a humidified incubator (Thermo, USA).

Reagents

The fluorogenic probe 2', 7'-dichlorofluorescein diacetate (DCFH-DA, D6883) was from Sigma. 5-bromo-2'-deoxyuridine (BrdU, 000103) was provided by Thermo Fisher Scientific. Anti-BrdU antibody (#5292S), anti-phospho-H3-S10 (#3377), anti-topoisomerase II α (#12286), anti-phospho-P53 (#9284), anti-P21(#2947), anti-CDK1(#9116), anti-phospho-CDK1(Tyr15) (#9111), anti-Cyclin B1(#4138), anti-PARP (#9542) and anti-Caspase 3 (#9662) were purchased from Cell Signaling Technology, anti-P53 (#AP6266d) was from Abcepta. Anti- β -Tubulin and anti-GAPDH antibodies were from Beijing TransGen Biotech (Beijing, China). Prestained Protein Ladder (26616) and M-PER buffer were from Thermo Pierce. FITC Annexin V Apoptosis Detection Kit I (#556547) and PI/RNase Staining Buffer (550825) were from BD Biosciences, protease inhibitor and phosphatase inhibitor cocktails were from Roche and the PVDF membrane was from Millipore.

9.4 T superconducting magnet and biological sample incubation system

The 9.4 T superconducting magnet with 100 mm diameter room temperature bore was custom-made by Xi An Superconducting Magnet Technology Company. We constructed two sets of incubation systems to fit the magnet (one for magnetic field exposure group, the other for sham group). The device consists of coaxial non-magnetic stainless-steel tubes. The outer diameter of the outer tube (OT) is 99 mm and the inner diameter of the inner tube (IT) is 87 mm. A non-magnetic stainless-steel sample house with 81 mm outer diameter was inserted into the inner space of the IT. A PT100 near the sample was used as a temperature sensor and connected to a temperature display to monitor the temperature of the sample. The temperature of the samples can be controlled

by water in the space between the IT and OT, and a solid-state relay was used to control the temperature of the water. By adjusting the temperature of the water, the temperature of the samples can be controlled precisely. To adjust the atmosphere of the sample house, the air (mice assays) or air with 5% CO₂ (cellular assays) was introduced through the air hole on the top. ANSYS WORKBENCH 14.0 software was used for device illustration in Fig. 1.

The superconducting magnet was designed to have a high degree of SMF homogeneity. The maximum magnetic field strength was at the magnet center. The homogeneity over 90 mm diameter in horizontal plane is within 2%, and that over 100 mm along vertical cylinder is within 4%. Our cell culture plates and mice were all in this region in this study, so the magnetic field induction values were within the range of 9–9.4 T.

Magnetic field exposure conditions for cells

The cells were plated on 35 mm cell culture plates at the density of 5×10^5 cells/mL, then treated with corresponding reagent and placed in the biological sample incubation system under 9.4 T SMFs or sham control for 24 h before they were harvested. The 9.4 T group was placed in the center of the 9.4 T superconducting magnet for stable magnetic field strength 24 h (with additional 3 h for increasing field and 1.5 h for reducing field). The sham control was placed in the other incubation tube, outside of the magnet and processed identically.

Xenograft tumor model in nude mice and magnetic field exposure

All animal experiments were strictly followed the National Institutes of Health guide for the care and use of Laboratory animals, animal experiments were reviewed and approved by animal ethics committee of Hefei institute of physical science, Chinese academy of sciences (Hefei, China), code DWLL-2019–25. 1×10^6 cells were injected subcutaneously into the right upper flank of the 6-week-old male BALB/c nude mouse (obtained from GemPharmatech Co.Ltd, China). Total of 24 mice bearing tumors about 2 mm in diameter were randomized into sham and 9.4 T SMFs groups ($n = 6$ for each group), which were exposed to upward or downward 9.4 T SMF for 8 h/day (11 a.m–7 p.m, with additional 3 h increasing field and 1.5 h reducing field), every other day, for 11 times (88 h) in total. Tumor diameters were measured with digital calipers, and the tumor volume in mm³ was calculated by $\text{Volume} = 0.5 \times \text{Length} \times (\text{Width})^2$. Food and water consumption were recorded every two days. In the end, all mice were euthanized through asphyxiation with an overdose of carbon dioxide gas and the tumor tissues were collected for further analysis. Plasma was collected for blood routine examination, and tissues were stained with hematoxylin-eosin for safety evaluation.

Measurement of intracellular ROS level

DCFH-DA was used as previously described [17]. Briefly, cells were harvested and mixed in pre-warmed DMEM without FBS, and with 5 μ M DCFH-DA for 30 min in the humidified incubator. Then the cells were washed and resuspended in PBS, and measured by flow cytometer (CytoFLEX, Beckman Coulter).

Cell counting and mitotic index analysis

Attached cells were trypsinized by 500 μ L trypsin and terminated by 500 μ L medium, then measured by flow cytometer (CytoFLEX, Beckman Coulter). For mitotic index measurement, cells were trypsinized and washed by PBS before they were fixed in 70% ice-cold ethanol overnight at –20 °C. Then the cells were washed and stained with phospho-Histone H3 (S10) at 1:1600 for 2.5 h at room temperature, washed twice by TBST and incubated with Alexa-488 conjugated anti-rabbit IgG. Then the cells were washed by TBST, resuspended in PBS, and analyzed by flow cytometer (CytoFLEX, Beckman Coulter).

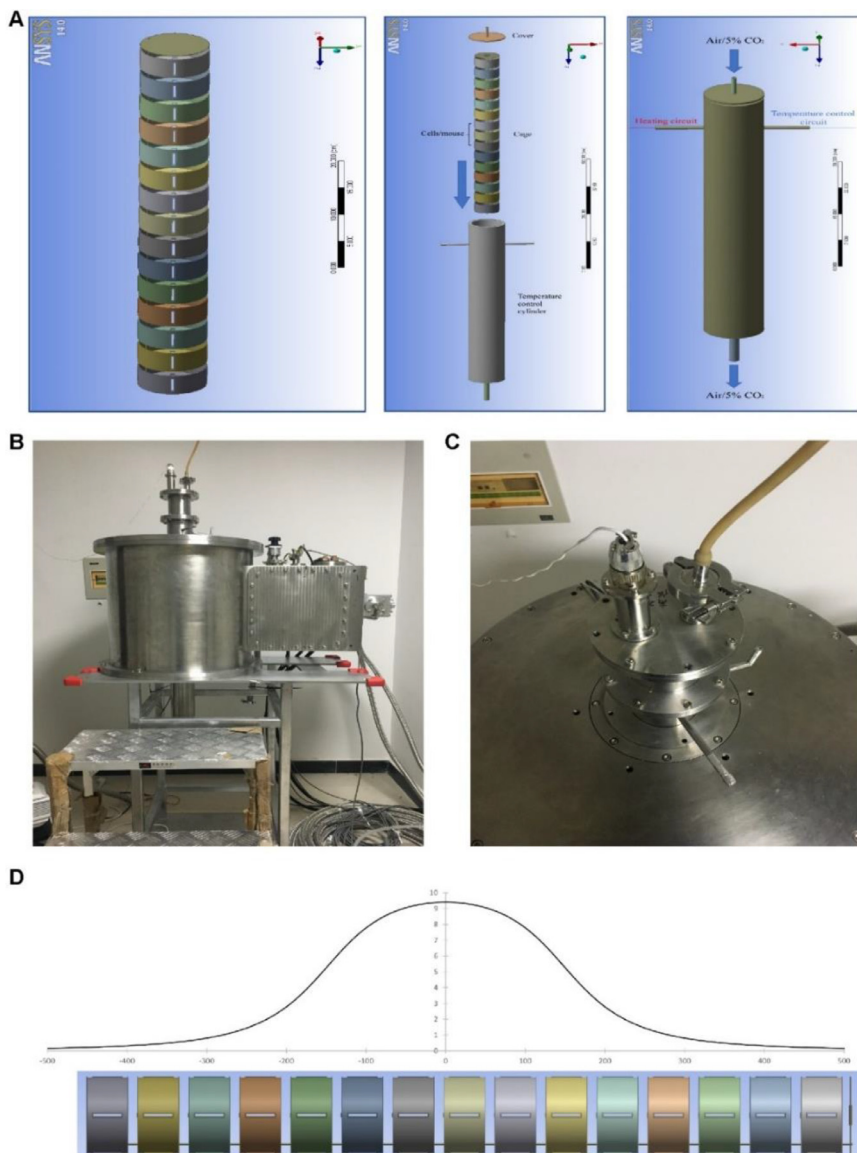


Fig. 1. 9.4 T superconducting magnet and the biological sample incubation system. (A) The diagram of culture tube device. Two identical sets were made. One was used in the magnet while the other was placed outside of the magnet to serve as the “sham” control. (B) The design and diagram of the biological sample incubation system. (C) Top view of the magnet with the biological sample incubation system inserted. (D) Distribution of the magnetic field induction (in T) along the long axis of the superconducting magnet.

Cell cycle distribution

Cells were trypsinized and washed by PBS before they were fixed in 70% ice-cold ethanol overnight at -20°C . Then cells were washed and incubated in PI solution in the dark at room temperature for 30 min. All the samples were measured by flow cytometry and analyzed by Modfit LT 5.0.

Cell death analysis

The FITC-Annexin V Apoptosis Detection Kit was used according to the manufacturer's instructions. Cells were trypsinized and washed by PBS before they were mixed in $100\ \mu\text{L}$ binding buffer with $5\ \mu\text{L}$ FITC-Annexin and $5\ \mu\text{L}$ propidium iodide (PI) in the dark at room temperature for 30 min. Then, $400\ \mu\text{L}$ binding buffer was added and analyzed by flow cytometry.

DNA synthesis assay

DNA synthesis assay was performed as previously described [12]. Briefly, cells were plated in 35 mm dish and treated with $10\ \mu\text{M}$ BrdU before they were exposed to 9.4 T SMF or sham at indicated time point.

Then all cells were harvested and washed by PBS, resuspended by 2 M HCl and incubated on the rotator for 30 min at room temperature. The cells were then centrifuged and resuspended by $0.1\ \text{M}\ \text{Na}_2\text{B}_4\text{O}_7$ (pH 8.5) at room temperature for 10 min before they were washed by PBS. Finally, the cells were incubated with anti-BrdU antibody for 2.5 h and the secondary Alexa Fluor 488 conjugated antibody for 1.5 h. All cells were analyzed by flow cytometry.

Western blotting

Cells were washed by PBS and lysed with M-PER supplemented with protease inhibitor and phosphatase inhibitor on ice for 40 min. Then all the lysate was mixed with $5\times$ SDS loading buffer and boiled at 98°C for 8 min. The samples were subjected to SDS-PAGE and transferred to PVDF membranes, which were blocked with 5% non-fat dried milk and incubated with indicated antibodies.

HE, Ki-67 and P53 staining

After the mice were sacrificed, their heart, liver, spleen, lung, kidney and tumor tissues were embedded and sectioned. Sections were deparaffinized and rehydrated with alcohol-xylene. For HE staining, the sections

were then stained with hematoxylin and eosin, scanned using a Panoramic DESK (3D HISTECH). For Ki-67 and P53 staining, sections were incubated in 3% H₂O₂ for 25 min to quench endogenous peroxidase activity before they were heated to retrieve the antigen. Then the sections were blocked with 3% BSA for 30 min at room temperature, incubated overnight at 4 °C with antibodies against Ki-67 (27309-1-ap, Proteintech) and P53 (GB13029-3, Servicebio). Histochemical kit (G1430, Servicebio) was used for immunohistochemical analysis. Sections staining were examined using CIC microscope.

Quantification and statistical analysis

Western blot bands were quantified by ImageJ software. For comparisons between groups, all the data had a normal distribution and were analyzed by a two-tailed Student's *t*-test. *P* values are labeled in the figures for where data were compared. For the data at different time points in the group, all of them had normal distributions and were analyzed by one-way ANOVA tests. All the statistical analysis was made by prism 8 software and *P* value < 0.05 was considered as statistically significant.

Results

A549 tumor growth in mice was significantly inhibited by the upward 9.4 T SMF

To investigate the biological effects of 9.4 T SMF, we constructed a set of incubation system to fit a superconducting magnet that could generate SMFs of up to 10 T (Fig. 1). The incubation system has 15 layers in total, with temperature and gas control. To achieve safety information for the future application of 9.4 T MRI in clinics, we set the magnet to 9.4 T, which means that the most center region of the magnet has 9.4 T SMF (Fig. 1A). To make sure that we have very accurate temperature control in this study, we only used the three layers in the center region, which provides 9.4 T SMF with minimum gradient. In addition, we also have a separate set of identical incubation system to be used as “sham control”, which has identical gas and temperature controls as the 9.4 T experimental set, but not inserted into the superconducting magnet. The only difference between the two sets is externally applied SMF. Furthermore, by switching the direction of electric current, we can change the direction of the SMF to be parallel or antiparallel to the gravity direction. In this way, we can compare the upward vs. downward SMFs for their effects on mice and cells.

To investigate the effect of 9.4 T SMF on lung cancer *in vivo*, we constructed lung cancer xenograft tumor model by injecting A549 cells subcutaneously into the right upper flank of nude mice. When the tumor diameter reached ~ 2 mm, the mice were randomly divided into different groups (*n* = 6) (Fig. 2A–B). The mice were exposed to sham or 9.4 T SMFs for 88 h in total (8 h/day, 11 times, every other day) in a 21-day period. The upward direction and downward direction were done on different days, with their own sham control groups. Food and water consumption, as well as body weight were measured every day. Consistent with our previous work [18], the water and food consumptions were not obviously affected by high field SMF exposure (Fig. 2C–D). The body weight was not affected either (Fig. 2E). However, the tumor growth was significantly inhibited by the upward 9.4 T SMF (Fig. 2F). At the end of 21 days, the tumor weight was reduced by the upward 9.4 T SMF by 44.7% (95%, CI:14.5–22.1%) (*P*<0.05) compared to the sham control (95%, CI:21–45.3%) (Fig. 2G). In contrast, the downward 9.4 T SMF did not inhibit the tumor growth (95%, CI:26.5–53.5%) (Fig. 2F–G). Therefore, magnetic field direction has significantly different effects *in vivo*, and the upward 9.4 T SMF can inhibit A549 tumor growth in mice.

Upward 9.4 T SMF inhibited DNA synthesis and caused cell cycle arrest

Next we examined the possible reasons that contributed to the tumor growth in 9.4 T upward SMF group. We first investigated the influence of 9.4 T SMF on A549 lung cancer cell proliferation by placing the cells in the center region of the superconducting magnet for 24 h (Fig. 3A). Our results show that the cell number of A549 was reduced significantly (31.2%, *P*<0.01) after 24 h upward 9.4 T treatment (Fig. 3B), which is much more significant than the 1 T or 0.5 T moderate SMF 48 h treatment in our previous studies (27.34% or 11.9%, *P* <0.05) [6]. Moreover, the cell number reduction only occurred in the upward 9.4 T, which is consistent with our previous finding that the upward direction SMFs could reduce some cancer cell number. We have also tested the cell numbers of two non-cancer cell lines, RPE1 and 293T cells, which were not significantly affected by 9.4 T SMFs (Fig. 3C).

Since reduced cell number can be the result of increased cell death, decreased cell proliferation, and/or cell cycle arrest, we first examined whether 9.4 T SMF treatment for 24 h could affect the A549 cell death. We used both Annexin/propidium iodide (PI) apoptosis assay by Flow cytometry and Western blot analysis with apoptosis markers, which showed that the upward and downward 9.4 T SMFs have no obvious influence on A549 cell death (Fig. 3C–E). We also used γ -H2AX, a commonly used marker for DNA damage and did not find obvious changes in DNA after 9.4 T SMF treatment (Fig. 3F).

Next, we examined cell proliferation. We used BrdU incorporation assay to measure DNA synthesis rates and found that DNA synthesis was significantly decreased by both upward (14.3%, *P* <0.01) and downward (18.6%, *P* <0.01) 9.4 T SMFs after 24 h (Fig. 4A). Our previous data shows that 1 T moderate SMF could inhibit DNA synthesis in HCT116, LoVo, PC9 and A549 cancer cells [12], but here we found that 0.5 T SMF has no effects on DNA synthesis (Fig. S1). Our previous data [12] also shows that 1 T moderate SMF has a combinational effect with the inhibitor of topoisomerase, a type of enzyme that resolves the tension of double strand DNA [19]. Here we used Western blot analysis to examine the level of TOP2 α (DNA topoisomerase II Alpha), which functions to bring the higher order compaction of chromatin to form condensed mitotic chromosomes during G2-M transition. Our results show that TOP2 α was decreased in both upward and downward 9.4 T SMF-treated cells (Fig. 4B).

The DNA synthesis inhibition by SMFs is likely due to the DNA supercoil changes through Lorenz forces on the negatively charged DNA in motion [12]. More specifically, we have previously proposed that the upward SMF could cause tightened DNA supercoils while the downward SMF causes loosen supercoils [12]. Interestingly, we found that the upward 9.4 T SMF significantly increased reactive oxygen species (ROS) level (Fig. 4C), a second messenger in many signaling pathways [20, 21], while the downward 9.4 T SMF did not (Fig. 4C). It is well known that ROS play central roles in multiple cellular processes, including triggering P53 activation, a key tumor suppressor. In fact, our data showed that the upward 9.4 T SMF could activate and upregulate P53 (Fig. 4D), but the downward 9.4 T SMF had no such effect (Fig. 4E), which is consistent with the ROS level changes. It is possible that the tightened DNA supercoils caused by Lorenz forces in upward 9.4 T SMF is a key step to boost ROS level, which consequently activate P53 and further inhibit DNA replication and cell proliferation.

Since reduced cell number can also be caused by cell cycle arrest, we next performed flow cytometry cell cycle analysis, which showed that the upward 9.4 T SMF slightly reduced the S phase and increased the G2/M population, while the downward 9.4 T SMF did not (Fig. 4F). Since the G2 and M phases are not distinguishable by PI staining alone, we used pH3 (S10), a mitotic cell marker, to probe M phase. Our results show that the mitotic index (% of mitotic cells) were decreased by both upward and downward 9.4 T treatments for 24 h (Fig. 4G). The fact that the G2/M phase was not much affected, but the mitotic index was decreased indicated that the G2 phase was likely

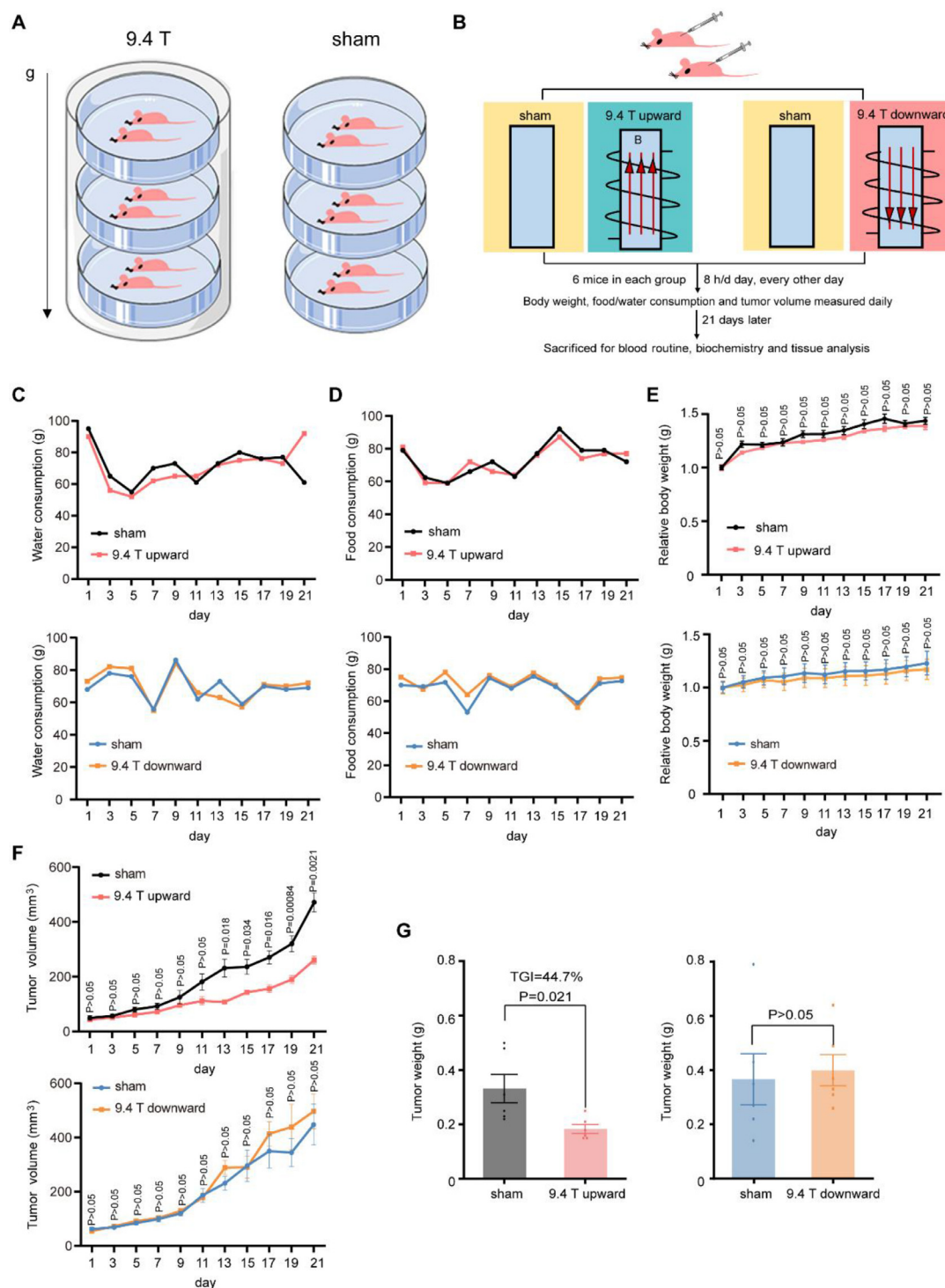


Fig. 2. A549 Tumor growth in mice were significantly inhibited by an upward 9.4 T SMF, but not downward direction. (A) Illustration of mice in 9.4 T SMF and sham condition. (B) Schematic illustration of the experiment procedure. (C) Water and (D) food consumption, as well as (E) relative body weight of mice exposed to sham and 9.4 T SMFs. There were six mice in every group, data are mean \pm SEM. (F) Tumor volume were measured each day for each mouse. (G) Tumor weight in sham, and 9.4 T magnetic field exposed groups at the end of 21 days.

to be prolonged. It is already known that cyclin dependent kinase 1 (CDK1) is inactivated by the phosphorylation on tyrosine 15 (Y15) during G2 phase and its dephosphorylation is required for CDK1 activation at G2-M boundary [22, 23]. Therefore, pCDK1(Y15) can be used as a G2 phase marker. In fact, our Western blot results showed that pCDK1(Y15) and cyclin B were both significantly increased by the upward 9.4 T SMF, but not downward 9.4 T (Fig. 4H). Therefore, the up-

ward 9.4 T SMF has reduced mitotic cells and arrested A549 cells at G2 phase.

The upward 9.4 T SMF has the potential to be a new anti-cancer treatment

The fact that the upward 9.4 T SMF is able to inhibit A549 tumor growth in mice and inhibit A549 cell proliferation *in vitro* indicate that

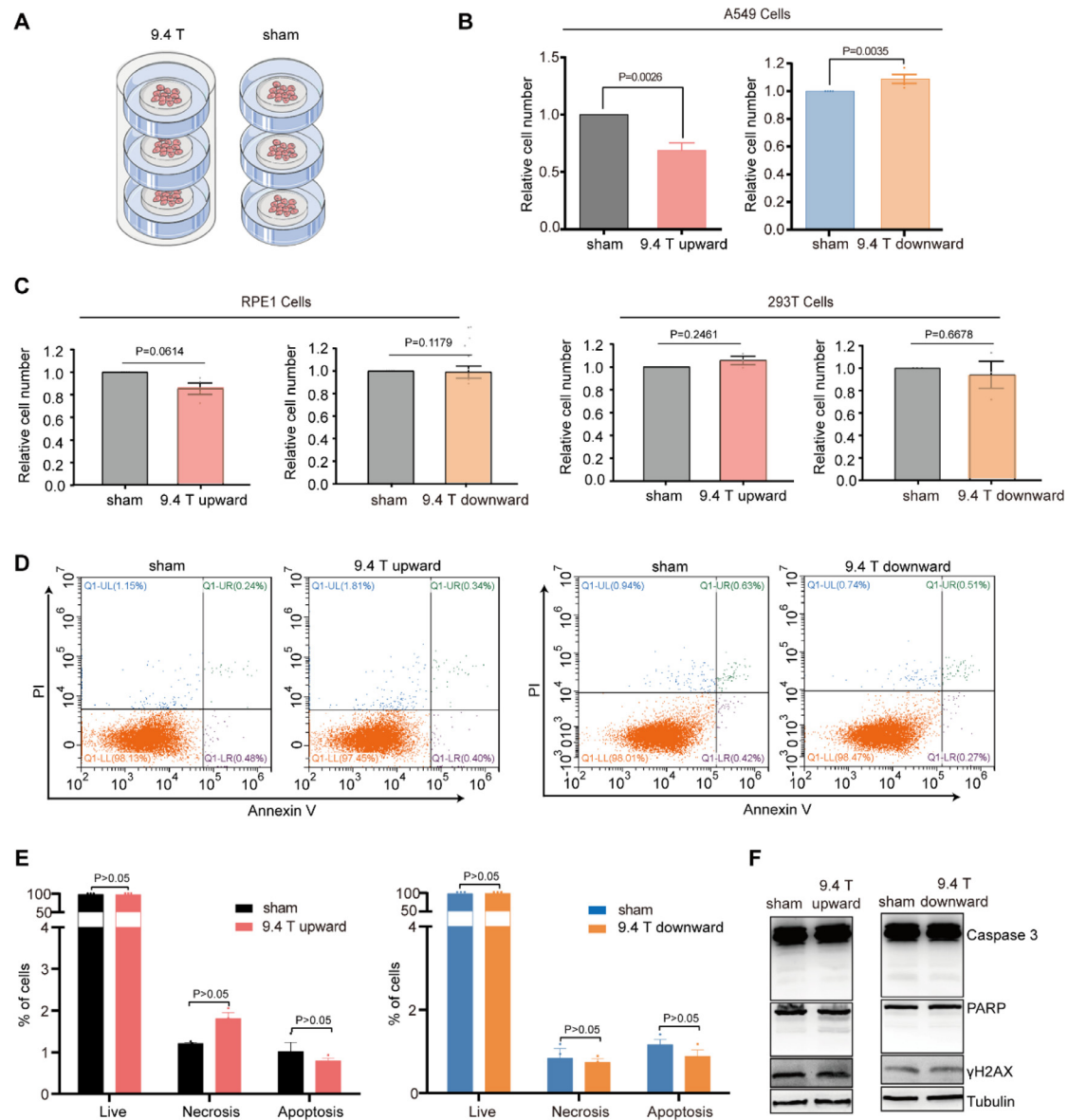


Fig. 3. Upward 9.4 T SMF significantly reduced cell number in A549 cells, but not downward direction. (A) The schematic diagram of cells in 9.4 T superconducting magnet and sham group. (B) Relative cell number of A549 cells exposed to 9.4 T SMFs for 24 h. (C) Relative cell number of RPE1 and 293T cells exposed to 9.4 T SMFs for 24 h. (D–E) The representative flow cytometry result of A549 cells exposed with 9.4 T SMFs and sham groups. (F) Western blots showed that 9.4 T SMFs treatment had no significant effect on apoptosis marker proteins (Caspases 3 and PARP) and DNA damage marker protein γ -H2AX in A549 cells.

it has anti-cancer potentials. Therefore, we performed basic physiological examinations on the SMF-treated mice besides the food/water consumption and body weight measurement to evaluate its safety issues. At the end of 21 days (total of 88 h), we performed tissue examinations and blood routine test. HE staining of the key organs (heart, liver, spleen, lung and kidney) did not reveal any obvious abnormalities (Fig. 5A). In addition, blood routine test showed that there were no obvious changes after 9.4 T SMF treatment (Fig. 5B–C). All the changes had no statistical significance. These results show that 9.4 T SMFs of both upward and downward directions did not generate tissue damage or severe defects on A549 tumor bearing mice.

To confirm the results we got *in vitro*, we further examined the tumor tissues of the mice treated with or without 9.4 T SMF for the tumor suppressor P53 and the proliferation marker Ki-67. It is obvious that the P53 level was significantly increased by the upward 9.4 T SMF, but not downward 9.4 T SMF (Fig. 6A–B). Moreover, the Ki-67 level was significantly decreased by the upward 9.4 T SMF, but not much by the

downward 9.4 T SMF (Fig. 6A–B). These are consistent with our findings that 9.4 T upward SMF could inhibit A549 lung cancer cell growth both *in vitro* and *in vivo*. Therefore, although both the upward and downward 9.4 T SMF could inhibit DNA synthesis *in vitro*, only the upward 9.4 T SMF can significantly increase ROS and P53 levels, decreased mitotic index and caused G2 cell arrest, which collectively lead to tumor growth inhibition in tumor bearing mice (Fig. 6C).

Discussion

The SMF intensities of MRI used in hospitals had increased from 1.5 T to 7 T [26–29]. Moreover, 9.4 T MRI has also been used in pre-clinical studies on healthy volunteers [4, 27], which is likely to be approved for clinics in the near future, as long as their safety issues are fully addressed. Our study here shows that 88 h of 9.4 T SMF treatment not only has no detrimental effects on A549 lung cancer bearing mice, but also have a significant tumor growth inhibition effect (TGI=44.7%,

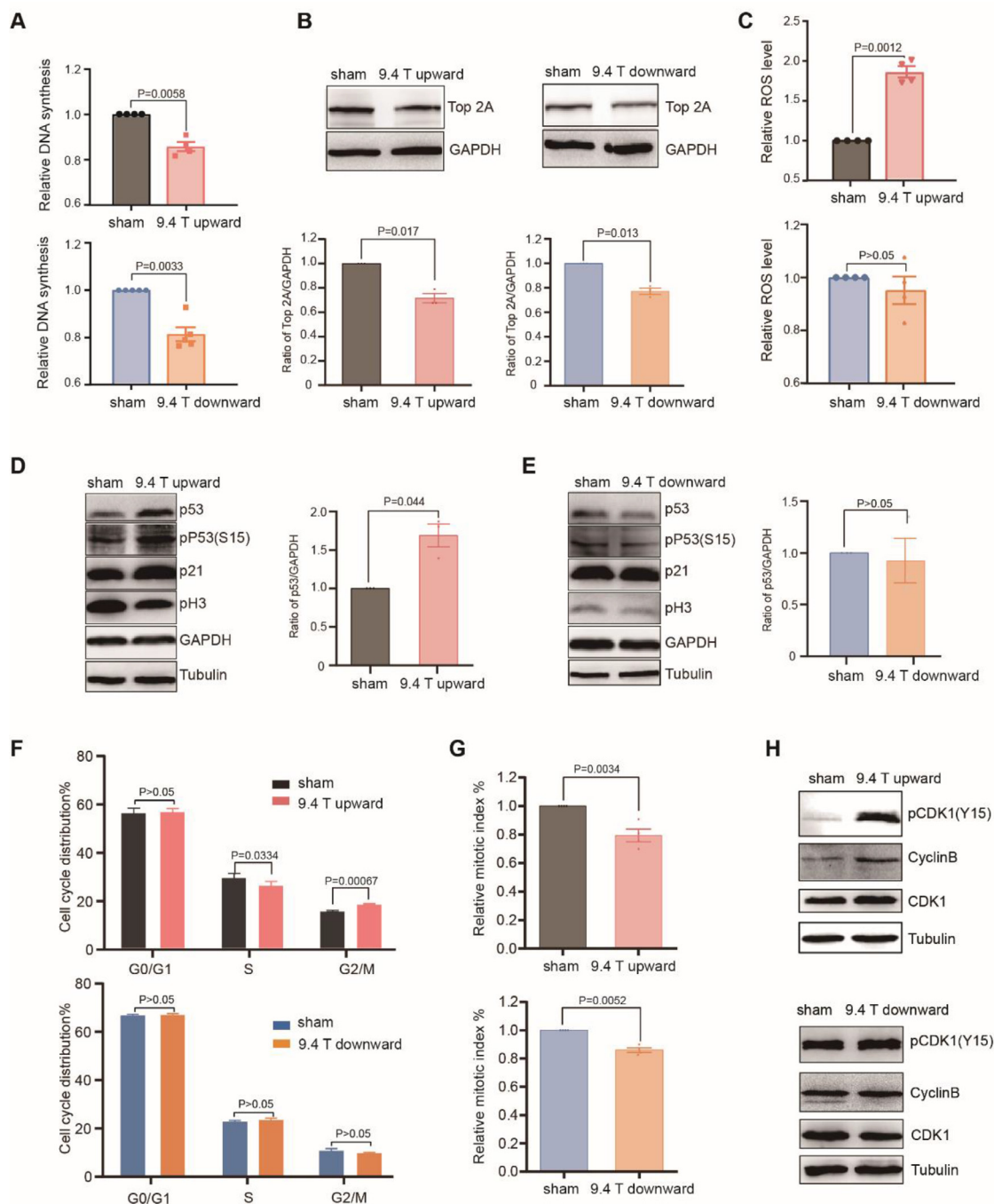


Fig. 4. Both 9.4 T SMFs significantly reduced mitotic index in A549 cells but only upward 9.4 T caused G2 arrest. (A) 9.4 T SMFs obviously inhibited the DNA replication of cells. (B) The level of Top 2 α treated with 9.4 T SMFs analyzed by Western blots and quantified by ImageJ software [24, 25]. (C) Upward 9.4 T SMF significantly increased the ROS levels of A549, but not downward. (D) Representative Western blots shows the level of phosphorylated P53 (S15) and P53 in the cells exposed with upward 9.4 T SMF were dramatically increased. (E) Representative Western blots shows the level of phosphorylated P53 (S15) and P53 in the cells exposed with downward 9.4 T SMF and statistical analysis for P53. (F) The representative flow cytometry result of cells exposed with 9.4 T SMFs that were stained by PI and analyzed by ModFit LT 5.0. (G) Flow cytometry analysis showed that both 9.4 T SMFs obviously decreased the expression of mitotic markers pH3(S10) in cell. (H) Upward 9.4 T SMF significantly inactivated the CDK1, but the phosphorylation level of CDK1 had no obvious change which treated by downward 9.4 T SMF.

$P < 0.05$) if the magnetic field direction is set to be vertically upward (Fig. 2G).

It should be mentioned that the mice were not under anesthesia in our study. They were fully awake and can move relatively freely in the chamber. Therefore, their whole bodies were exposed to the magnetic field. One of the goals of this study was also to investigate the potential safety issues of 9.4 T magnetic field long-term exposure be-

cause 9.4 T high-field MRI is currently in preclinical trials, which needs more studies for its safety before their future clinical application. Our results show that mice whole body long-term exposure to 9.4 T does not cause detrimental effects, which provides very useful basis for human studies.

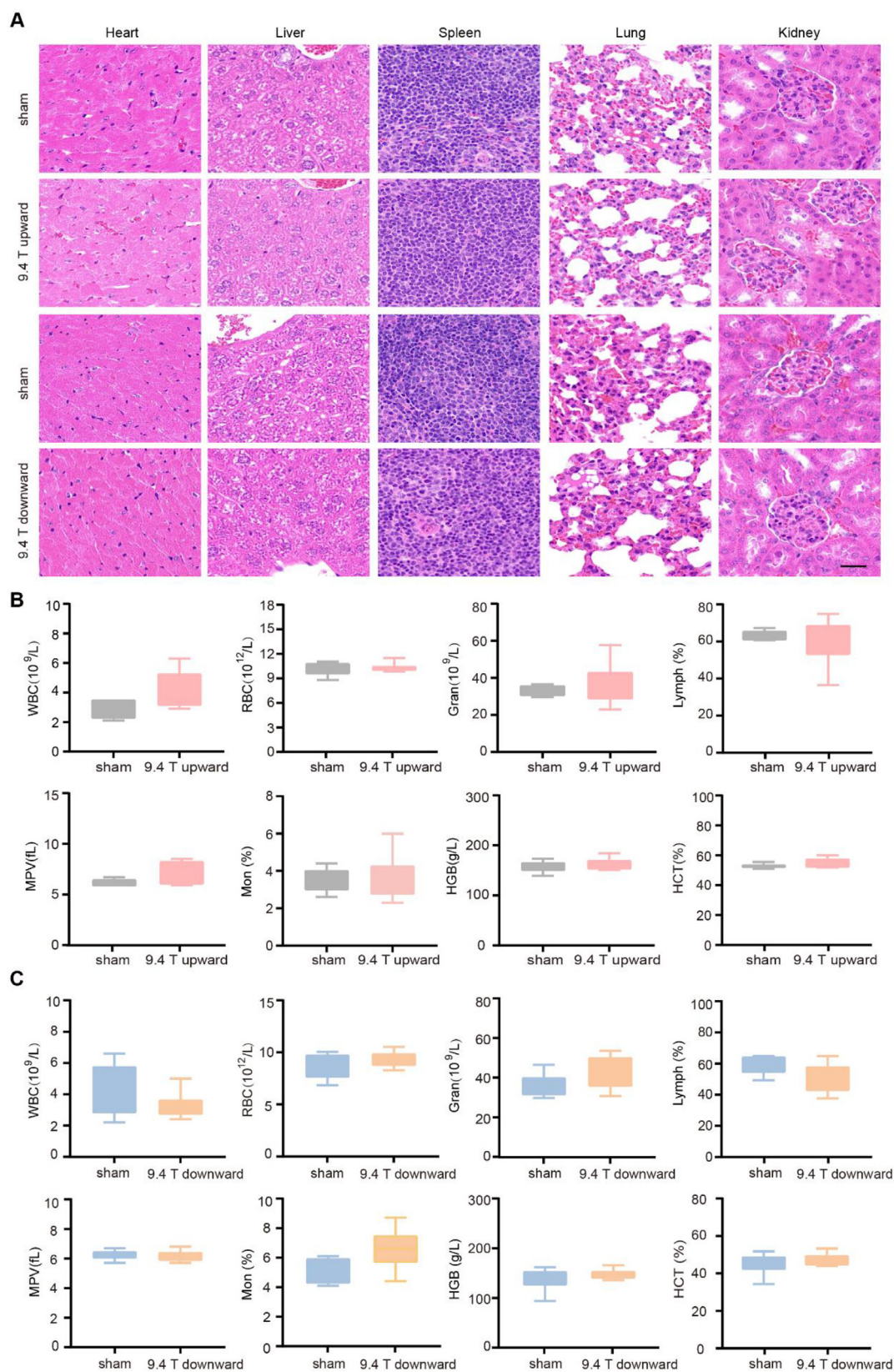


Fig. 5. The upward 9.4 T SMF does not have severe effects on vital parameters of tumor-bearing mice. **(A)** HE stains of heart, liver, spleen, lung, and kidney in sham and 9.4 T SMFs treatment groups. Scale bar: 50 μ m. **(B, C)** Blood routine examination of mice exposed sham and upward or downward 9.4 T SMF. Comparisons were made between sham and 9.4 T group. There were six mice in each group, values show mean \pm SEM. We did statistical analysis for all data, and all of them had no statistical significance ($P > 0.05$).

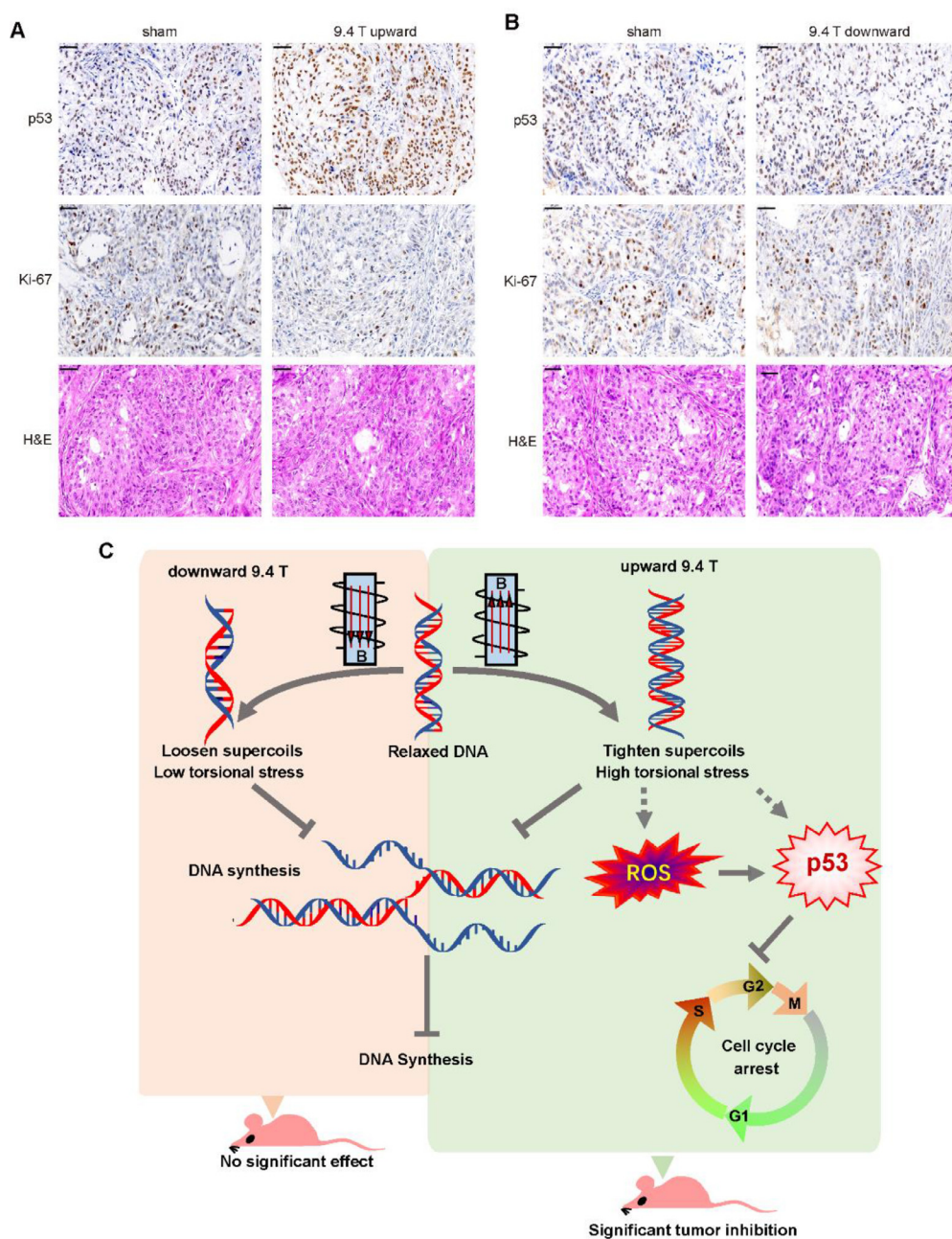


Fig. 6. 9.4 T SMF increased P53 level and decreased Ki-67 level in mice tumor tissues. Representative images of P53 and Ki-67 immunohistochemistry staining or HE staining of sham, (A) upward 9.4 T SMF or (B) downward 9.4 T SMF treated mice tumor tissues. Scale bar: 50 μ m. (C) The model of 9.4 T magnetic fields influence the cell number of A549 lung cancer cells.

Magnetic field direction and biological effects

It was very interesting but still puzzling that the SMF direction can produce differential biological effects [6, 14, 15, 30]. Back in 1974, a book [Ref?] claimed that the N and S poles of a permanent magnet can induce different effects on living systems, but no experimental evidences were provided [30]. Our previous data also showed that upward 0.2–1 T SMF could reduce the cell number of multiple human cancer cells and obviously inhibited GIST-T1 tumor growth in mice, while the downward SMF did not [6]. Recently, we showed that 1 T upward SMF could inhibit DNA synthesis of A549, PC9, HCT116 and LoVo cells but not 1 T downward SMF [12]. We hypothesized that the SMF could align DNA chains and exert the Lorentz forces on negative charges of DNA, which differentially affected the DNA rotation and supercoil tightness [12]. Similarly, in this study, 9.4 T SMFs of both upward and downward directions inhibited DNA synthesis, which was likely due to the fact that the Lorentz force acted on the DNA strands in both cases were strong

enough to perturb the DNA conformation, which further affected DNA synthesis (Fig. 6C).

One puzzling issue we cannot explain is the fact that the downward 9.4 T SMF could inhibit DNA synthesis, but the cell number was not reduced. It has been reported that the S-phase cells would be forced to enter mitosis directly without completing DNA synthesis in some cases [31]. We speculate that downward 9.4 T SMF may have similar effect and accelerated cell cycle, which cancels out the effect of DNA synthesis inhibition on cell proliferation. Furthermore, we found that A549 lung cancer growth both *in vitro* and *in vivo* were suppressed only by upward 9.4 T SMF, through activating the ROS-P53 pathway.

SMF and ROS-P53

ROS are a series of highly active free radical, ions and molecules that have unpaired electrons in their outermost electron orbit [7]. The effects of different MFs on ROS are variable, which largely depends on MF pa-

parameters and biological samples examined [32]. Although some studies have found that weak to moderate intensity SMFs could reduce the ROS level in multiple cell lines and during planarian blastema regeneration [17, 33], the effects of high SMFs on ROS levels are poorly studied. Our results here show that the upward direction 9.4 T SMF exposure for 24 h can increase cellular ROS in A549 cells by 2-fold (Fig. 4C). However, since the SMFs we used have minimum gradient, which is likely the reason why they did not produce as significant ROS level increase as large gradient SMFs [34]. It seems that the 2-fold ROS level increase generated by 9.4 T upward SMF is not high enough to trigger apoptosis in A549 cells (Fig. 3D).

However, it is interesting that the upward 9.4 T SMF can significantly increase the level of P53 (Fig. 4D). It is known that ROS can trigger P53 activation and have an inextricable relationship with P53 [35]. As an essential antitumor protein, P53 plays a key role in maintaining genomic integrity, stress response, induce cell cycle arrest, senescence or apoptosis through activating different target genes [36], which has been shown by two previous studies that it can be affected by some dynamic MFs [37, 38]. For SMFs, there was a study using a neodymium magnetic disk with south pole facing up, which provided an inhomogeneous 6 mT downward direction SMF, affected P53 location in aged lymphocytes [39]. More importantly and interestingly, it has been shown that increased DNA supercoiling can significantly increase the binding of P53 to DNA [40, 41]. Therefore, we hypothesize that SMF-induced DNA supercoil tightness may not only increase P53 through ROS elevation, but also directly increase P53 binding through DNA topology changes (Fig. 6C).

SMF and DNA synthesis

The effect of SMFs on DNA synthesis has been examined in a few studies, but was not conclusive in the literature, which is mainly due to the different parameters and experimental conditions. For example, it had been reported that 1 h 1.5 T SMF exposure for three times a week slightly inhibited fetal lung fibroblast cell DNA synthesis after the first and third week (about 5% and 4%), but after the second week, the DNA synthesis was increased by 12% [42]. Recently, we found that upward and downward 1 T SMFs differentially inhibited the DNA synthesis of A549, PC9, HCT116 and LoVo cells [12]. Apparently, cell types can directly affect the outcomes of SMF on DNA synthesis [43–45]. Here we found that the DNA synthesis was significantly decreased by both upward (14.3%) and downward (18.6%) 9.4 T SMFs after 24 h (Fig. 4A). Since the negatively charged DNA strands intrinsically rotate during DNA unwinding, replication and transcription in cells, the tightness of DNA supercoils could theoretically be affected by SMF through the Lorentz forces acting on the moving charges, and DNA synthesis would consequently be affected [12]. Therefore, SMF intensity and direction as well as cell types can directly affect the outcomes of an SMF, which will need further investigations.

Conclusion

In summary, our study shows that 88 h of 9.4 T SMF treatment does not have harmful effects on A549 lung cancer bearing mice, and the upward 9.4 T SMF significantly inhibits A549 lung cancer growth. This not only provides useful information for the future clinical application of 9.4 T MRI in the near future, especially on patients with diseases including cancer, but also reveals that 9.4 T SMF upward direction has the potential to be developed as an anti-cancer treatment in the future.

Declaration of Competing Interest

The authors declare that they have no conflict of interest.

CRediT authorship contribution statement

Xingxing Yang: Data curation, Formal analysis, Investigation, Software, Methodology, Writing - original draft, Writing - review & edit-

ing. **Chao Song:** Data curation, Formal analysis, Investigation, Software, Methodology, Writing - original draft. **Lei Zhang:** Data curation, Formal analysis, Investigation, Software, Methodology, Writing - original draft. **Junjun Wang:** Investigation, Writing - original draft. **Xin Yu:** Investigation, Writing - original draft. **Biao Yu:** Investigation, Writing - original draft. **Vitalii Zablotskii:** Conceptualization, Methodology, Writing - original draft. **Xin Zhang:** Conceptualization, Project administration, Funding acquisition, Methodology, Supervision, Writing - original draft, Writing - review & editing.

Funding

Project was supported by the National Key R&D Program of China (Grant No. 2016YFA0400900), National Natural Science Foundation of China (31900506), the CASHIPS Director's Fund (YZJJ201704 and KP-2017-26), Heye Health Technology Foundation (HYJJ20190801), the National Science Foundation for Young Scientists of China (31900506) and the National Science Foundation of Anhui Province (1908085MA11), China Postdoctoral Science Foundation Funded Project (2019M652222).

Supplementary materials

Supplementary material associated with this article can be found, in the online version, at doi:10.1016/j.tranon.2021.101103.

References

- [1] I.C. Atkinson, K.R. Thulborn, Feasibility of mapping the tissue mass corrected bioscale of cerebral metabolic rate of oxygen consumption using 17-oxygen and 23-sodium MR imaging in a human brain at 9.4T, *NeuroImage* 51 (2010) 723–733.
- [2] M. Timme, M. Masthoff, N. Nagelmann, M. Masthoff, C. Faber, S. Bürklein, Imaging of root canal treatment using ultra high field 9.4T UTE-MRI – a preliminary study, *Dentomaxillofac. Radiol.* 49 (2020) 20190183.
- [3] T. Vaughan, L. DelaBarre, C. Snyder, J. Tian, C. Akgun, D. Shrivastava, W. Liu, C. Olson, G. Adriany, J. Strupp, P. Andersen, A. Gopinath, P.F. van de Moortele, M. Garwood, K. Ugurbil, 9.4 T human MRI: preliminary results, *Magn. Reson. Med.* 56 (2006) 1274–1282.
- [4] J. Bause, P. Ehse, C. Mirkes, G. Shajan, K. Scheffler, R. Pohmann, Quantitative and functional pulsed arterial spin labeling in the human brain at 9.4 T, *Magn. Reson. Med.* 75 (2016) 1054–1063.
- [5] L. Zhang, X. Ji, X. Yang, X. Zhang, Cell type- and density-dependent effect of 1 T static magnetic field on cell proliferation, *Oncotarget* 8 (2017) 13126–13141.
- [6] X. Tian, D. Wang, M. Zha, X. Yang, X. Ji, L. Zhang, X. Zhang, Magnetic field direction differentially impacts the growth of different cell types, *Electromagn. Biol. Med.* 37 (2018) 114–125.
- [7] X. Zhang, K. Yarema, A. Xu, *Biological Effects of Static Magnetic Fields*, Springer, 2017.
- [8] T. Higashi, A. Yamagishi, T. Takeuchi, N. Kawaguchi, S. Sagawa, S. Onishi, M. Date, Orientation of erythrocytes in a strong static magnetic field, *Blood* 82 (1993) 1328–1334.
- [9] A. Prina-Mello, E. Farrell, P. Prendergast, V. Campbell, J. Coey, Influence of strong static magnetic fields on primary cortical neurons, *Bioelectromagn. J. Bioelectromagn. Soc., Soc. Phys. Regul. Biol. Med. Eur. Bioelectromagn. Assoc.* 27 (2006) 35–42.
- [10] L. Zhang, J. Wang, H. Wang, W. Wang, Z. Li, J. Liu, X. Yang, X. Ji, Y. Luo, C. Hu, Y. Hou, Q. He, J. Fang, J. Wang, Q. Liu, G. Li, Q. Lu, X. Zhang, Moderate and strong static magnetic fields directly affect EGFR kinase domain orientation to inhibit cancer cell proliferation, *Oncotarget* 7 (2016) 41527–41539.
- [11] L. Zhang, Y. Hou, Z. Li, X. Ji, Z. Wang, H. Wang, X. Tian, F. Yu, Z. Yang, L. Pi, T.J. Mitchison, Q. Lu, X. Zhang, Correction: 27 T ultra-high static magnetic field changes orientation and morphology of mitotic spindles in human cells, *Elife* 6 (2017) e28212.
- [12] X. Yang, Z. Li, T. Polyakova, A. Dejneka, V. Zablotskii, X. Zhang, Effect of static magnetic field on DNA synthesis: the interplay between DNA chirality and magnetic field left-right asymmetry, *FASEB bioAdvances* 2 (2020) 254–263.
- [13] Y. Jin, W. Guo, X. Hu, M. Liu, X. Xu, F. Hu, Y. Lan, C. Lv, Y. Fang, M. Liu, Static magnetic field regulates Arabidopsis root growth via auxin signaling, *Sci. Rep.* 9 (2019) 1–14.
- [14] I.D. Milovanovich, S. Ćirković, S.R. De Luka, D.M. Djordjević, A.Ž. Ilić, T. Popović, A. Arsić, D.D. Obradović, D. Oprić, J.L. Ristić-Djurović, A.M. Trbović, Homogeneous static magnetic field of different orientation induces biological changes in subcutaneously exposed mice, *Environ. Sci. Pollut. Res.* 23 (2016) 1584–1597.
- [15] S.R. De Luka, A.Ž. Ilić, S. Janković, D.M. Djordjević, S. Ćirković, I.D. Milovanovich, S. Stefanović, S. Veskić-Moračanin, J.L. Ristić-Djurović, A.M. Trbović, Sub-chronic exposure to static magnetic field differently affects zinc and copper content in murine organs, *Int. J. Radiat. Biol.* 92 (2016) 140–147.

- [16] S. Hapuarachchige, Y. Kato, E.J. Ngen, B. Smith, M. Delannoy, D. Artemov, Non-temperature induced effects of magnetized iron oxide nanoparticles in alternating magnetic field in cancer cells, *PLoS One* 11 (2016) e0156294.
- [17] H. Wang, X. Zhang, ROS reduction does not decrease the anticancer efficacy of X-ray in two breast cancer cell lines, *Oxid. Med. Cell Longev.* 2019 (2019) 3782074.
- [18] X. Tian, D. Wang, S. Feng, L. Zhang, X. Ji, Z. Wang, Q. Lu, C. Xi, L. Pi, X. Zhang, Effects of 3.5–23.0 T static magnetic fields on mice: a safety study, *NeuroImage* 199 (2019) 273–280.
- [19] Y. Pommier, Y. Sun, N.H. Shar-yin, J.L. Nitiss, Roles of eukaryotic topoisomerases in transcription, replication and genomic stability, *Nat. Rev. Mol. Cell Biol.* 17 (2016) 703.
- [20] L.S. Terada, Specificity in reactive oxidant signaling: think globally, act locally, *J. Cell Biol.* 174 (2006) 615–623.
- [21] A. Takahashi, N. Ohtani, K. Yamakoshi, S.-i. Iida, H. Tahara, K. Nakayama, K.I. Nakayama, T. Ide, H. Saya, E. Hara, Mitogenic signalling and the p16INK4a-Rb pathway cooperate to enforce irreversible cellular senescence, *Nat. Cell Biol.* 8 (2006) 1291–1297.
- [22] R.N. Booher, P.S. Holman, A. Fattaey, Human Myt1 is a cell cycle-regulated kinase that inhibits Cdc2 but not Cdk2 activity, *J. Biol. Chem.* 272 (1997) 22300–22306.
- [23] W.R. Taylor, G.R. Stark, Regulation of the G2/M transition by p53, *Oncogene* 20 (2001) 1803–1815.
- [24] K.M. Wylie, J.E. Schrimpf, L.A. Morrison, Increased eIF2 α phosphorylation attenuates replication of herpes simplex virus 2 vhs mutants in mouse embryonic fibroblasts and correlates with reduced accumulation of the PKR antagonist ICP34.5, *J. Virol.* 83 (2009) 9151.
- [25] V. Marcel, S.E. Ghayad, S. Belin, G. Therizols, A.-P. Morel, E. Solano-González, J.A. Vendrell, S. Hacot, H.C. Mertani, M.A. Albaret, J.-C. Bourdon, L. Jordan, A. Thompson, Y. Tafer, R. Cong, P. Bouvet, J.-C. Saurin, F. Catez, A.-C. Prats, A. Puisieux, J.-J. Diaz, p53 Acts as a safeguard of translational control by regulating fibrillarin and rRNA methylation in cancer, *Cancer Cell* 24 (2013) 318–330.
- [26] C. Park, C. Kang, Y. Kim, Z. Cho, Advances in MR angiography with 7T MRI: from microvascular imaging to functional angiography, *NeuroImage* 168 (2018) 269–278.
- [27] K. Uğurbil, The road to functional imaging and ultrahigh fields, *NeuroImage* 62 (2012) 726–735.
- [28] O. Kraff, H.H. Quick, 7T: physics, safety, and potential clinical applications, *J. Magn. Reson. Imaging* 46 (2017) 1573–1589.
- [29] M.E. Ladd, P. Bachert, M. Meyerspeer, E. Moser, A.M. Nagel, D.G. Norris, S. Schmitter, O. Speck, S. Straub, M. Zaiss, Pros and cons of ultra-high-field MRI/MRS for human application, *Prog. Nucl. Magn. Reson. Spectrosc.* 109 (2018) 1–50.
- [30] A.R. Davis, W.C. Rawls, in: *Magnetism and its Effects on the Living System*, Exposition Press, 1974, p. 1974.
- [31] M. Aarts, R. Sharpe, I. Garcia-Murillas, H. Gevensleben, M.S. Hurd, S.D. Shumway, C. Toniatti, A. Ashworth, N.C. Turner, Forced mitotic entry of S-phase cells as a therapeutic strategy induced by inhibition of WEE1, *Cancer Discov.* 2 (2012) 524–539.
- [32] H. Wang, X. Zhang, Magnetic fields and reactive oxygen species, *Int. J. Mol. Sci.* 18 (2017) 2175.
- [33] A.V. Van Huizen, J.M. Morton, L.J. Kinsey, D.G. Von Kannon, M.A. Saad, T.R. Birkholz, J.M. Czajka, J. Cyrus, F.S. Barnes, W.S. Beane, Weak magnetic fields alter stem cell-mediated growth, *Sci. Adv.* 5 (2019) eaau7201.
- [34] V. Zablotskii, T. Polyakova, A. Dejneka, Cells in the non-uniform magnetic world: how cells respond to high-gradient magnetic fields, *Bioessays* 40 (2018) e1800017.
- [35] B. Liu, Y. Chen, D.K. St Clair, ROS and p53: a versatile partnership, *Free Radic. Biol. Med.* 44 (2008) 1529–1535.
- [36] G. Liu, X. Chen, Regulation of the p53 transcriptional activity, *J. Cell. Biochem.* 97 (2006) 448–458.
- [37] P. Solek, L. Majchrowicz, D. Bloniarz, E. Krotoszynska, M. Koziarowski, Pulsed or continuous electromagnetic field induce p53/p21-mediated apoptotic signalling pathway in mouse spermatogenic cells *in vitro* and thus may affect male fertility, *Toxicology* 382 (2017) 84–92.
- [38] J. Ren, L. Ding, Q. Xu, G. Shi, X. Li, X. Li, J. Ji, D. Zhang, Y. Wang, T. Wang, Y. Hou, LF-MF inhibits iron metabolism and suppresses lung cancer through activation of P53-miR-34a-E2F1/E2F3 pathway, *Sci. Rep.* 7 (2017) 749.
- [39] B. Tenuzzo, C. Vergallo, L. Dini, Effect of 6mT static magnetic field on the bcl-2, bax, p53 and hsp70 expression in freshly isolated and *in vitro* aged human lymphocytes, *Tissue Cell* 41 (2009) 169–179.
- [40] E. Paleček, D. Vlč, V. Staňková, V. Brázda, B. Vojtěšek, T.R. Hupp, A. Schaper, T.M. Jovin, Tumor suppressor protein p53 binds preferentially to supercoiled DNA, *Oncogene* 15 (1997) 2201–2209.
- [41] Eva B. Jagelská, V. Brázda, P. Pečinka, E. Paleček, M. Fojta, DNA topology influences p53 sequence-specific DNA binding through structural transitions within the target sites, *Biochem. J.* 412 (2008) 57–63.
- [42] J. Wiskirchen, E. Groenewaller, R. Kehlbach, F. Heinzlmann, M. Wittau, H. Rodemann, C. Claussen, S. Duda, Long-term effects of repetitive exposure to a static magnetic field (1.5 T) on proliferation of human fetal lung fibroblasts, *Magn. Reson. Med.* 41 (1999) 464–468.
- [43] F.Q. Ngo, J.W. Blue, W.K. Roberts, The effects of a static magnetic field on DNA synthesis and survival of mammalian cells irradiated with fast neutrons, *Magn. Reson. Med.* 5 (1987) 307–317.
- [44] K. Sato, H. Yamaguchi, H. Miyamoto, Y. Kinouchi, Growth of human cultured cells exposed to a non-homogeneous static magnetic field generated by Sm-Co magnets, *Biochim. ET Biophys. Acta-Mol. Cell Res.* 1136 (1992) 231–238.
- [45] L. Qiu, X. Tang, M. Zhong, Z. Wang, Effect of static magnetic field on proliferation and cell cycle of osteoblast cell, *Shanghai Kou Qiang Yi Xue* 13 (2004) 469–470.